

Received: 2019.11.21
Accepted: 2019.12.18
Available online: 2020.01.22
Published: 2020.03.10

Downregulated Long Non-Coding RNA MSC-AS1 Inhibits Osteosarcoma Progression and Increases Sensitivity to Cisplatin by Binding to MicroRNA-142

Authors' Contribution:
Study Design A
Data Collection B
Statistical Analysis C
Data Interpretation D
Manuscript Preparation E
Literature Search F
Funds Collection G

ACDF 1 **Longqiang Zhang***
ABDF 1 **Guangzong Zhao***
CD 1 **Shaolin Ji**
DEF 1 **Qihua Yuan**
F 2 **Haiyan Zhou**

1 Department of Orthopedics, Yidu Central Hospital of Weifang, Weifang, Shandong, P.R. China
2 Health Management Center, Weifang People's Hospital, Weifang, Shandong, P.R. China

Corresponding Author:
Source of support:

* Longqiang Zhang and Guangzong Zhao contributed equally to this work
Haiyan Zhou, e-mail: Zhouhaiyan08151@163.com
Departmental sources

Background: Osteosarcoma (OS) is the most prevalent malignant primary bone tumor, resulting from severe transformation of primitive mesenchymal cells, which induces osteogenesis. Long non-coding RNA (lncRNA) MSC-AS1 triggers osteogenic differentiation by sponging microRNA (miR)-140-5p. The present study assessed the mechanism of lncRNA MSC-AS1 in OS biological features and sensitivity to cisplatin (DDP) by binding to miR-142.





Material/Methods: Firstly, lncRNA MSC-AS1 expression in OS tissues and cells was analyzed. OS cells were transfected with silenced MSC-AS1 to determine its role in OS biological behaviors, and we also assessed the effect of MSC-AS1 on OS sensitivity to DDP. Then, website prediction and dual-luciferase reporter gene assay were utilized for verification of the binding site between MSC-AS1 and miR-142. Reverse transcription-quantitative polymerase chain reaction (RT-qPCR) and Western blot analysis were performed to determine the effect of MSC-AS1 on expression of miR-142, cyclin-dependent kinase 6 (CDK6), and the PI3K/AKT signaling pathway. Xenograft transplantation was also applied to confirm the *in vitro* experiments.

Results: Overexpressed MSC-AS1 was associated with poor prognosis of OS patients. OS cell proliferation, invasion, and migration were reduced after silencing MSC-AS1, while cell apoptosis was enhanced. Moreover, silencing MSC-AS1 made OS cells more sensitive to DDP. Interestingly, MSC-AS1 knockdown induced miR-142 expression and reduced CDK6 levels, thereby decreasing the protein expression of p-PI3K/t-PI3K and p-AKT/t-AKT. Silencing MSC-AS1 repressed OS progression *in vivo*.

Conclusions: Our study demonstrated that silencing MSC-AS1 inhibited OS biological behaviors by enhancing miR-142 to decrease CDK6 and inactivating the PI3K/AKT axis. Our results may provide new insights for OS treatment.

MeSH Keywords: **Cisplatin • Cyclin-Dependent Kinase 6 • MicroRNAs • Osteosarcoma**

Full-text PDF: <https://www.medscimonit.com/abstract/index/idArt/921594>

 3582  2  5  35



Background

Osteosarcoma (OS) is the most common primary bone cancer, with multiple genomic aberrations and mesenchymal cells, generating malignant osteoid or immature bones [1,2]. OS, which is mostly found in long bones, is most common in children, and is also common in the elderly [3]. The exact cause of OS is unknown, but risk factors for OS are both environmental and inherently, including radiation damage and genetic disorders [4]. Amputation, limb-sparing operations, palliative radiation, and bone resorption inhibition therapies are currently used treatments for OS [5]. However, although the adjusted strategic management has stabilized the 10-year survival rates to 50% in the past few decades, there has been little improvement in OS survival rates [6]. Cisplatin (DDP) has emerged as an important and effective OS treatment [7], but novel therapeutic strategies for OS are urgently needed. Therefore, the present study focused on use of long non-coding RNA (lncRNA) to understand the underlying mechanism in OS development in order to develop novel intervention strategies.

lncRNAs are important in disease occurrence and development, and their associations with these diseases suggest new perspectives on the pathogenesis, diagnosis, and treatment of diseases [8]. Many upregulated lncRNAs have been found to be oncogenic factors in OS malignancy [9]. In addition, a recent study found that lncRNA MSC-AS1 is overexpressed in pancreatic ductal adenocarcinoma (PDAC), which leads to poor prognosis [10]. Our research found that MSC-AS1 binds to microRNA (miR)-142; miRs are major participants in a wide range of cancer cell biological behaviors, including OS [11]. As a tumor inhibitor gene, miR-142 overexpression greatly hinders OS cell proliferation [12]. We previously reported there is a binding site between miR-142 and cyclin-dependent kinase 6 (CDK6), which has important roles in tumor cell transcription and hematopoietic stem cells [13]. Zhu et al. found that miR-29b can target CDK6 to curb OS processes [14]. In addition, the activated phosphatidylinositol 3-kinase (PI3K)/protein kinase B (AKT) signaling pathway serves as an oncogene in many cancers by expediting cell proliferation [15]. In a previous study, inhibition of the PI3K/AKT signaling pathway was shown to repress OS processes [16]. Taken together, the evidence presented above suggests there may be interactions between lncRNA MSC-AS1 and miR-142 in OS biological behaviors and cell sensitivity to cisplatin (DDP). Thus, we conducted the present series of experiments to test this hypothesis.

Material and Methods

Ethics statement

This study was supervised and approved by the Ethics Committee of Yidu Central Hospital in Weifang. All the subjects

provided signed informed consent. All procedures in this study were approved by our institution's Laboratory Animal Ethics Committee.

Clinical samples

From March 2014 to June 2018, 45 OS patients who underwent surgery at Yidu Central Hospital in Weifang were enrolled in this study and we obtained samples of OS tissues and adjacent normal bone tissues. These patients were followed up for 5 years.

Cell cultivation

Human normal osteoblast hFOB1.19 cells and OS cell lines MG63, SOSP-9607, HOS, U2OS, and SaOS2 were purchased from Shanghai Institute of Biochemistry and Cell Biology, Chinese Academy of Sciences (Shanghai, China) and were cultivated in Dulbecco's modified Eagle's medium (DMEM) consisting of 10% fetal bovine serum (FBS) in a 37°C incubator with 5% CO₂. DMEM was changed every 2 to 3 days. The cells were detached and subcultured when cell confluence reached 80%.

U2OS cells (1×10⁵ cells/mL) in logarithmic growth phase were inoculated on 6-well plates and cultured with high-glucose DMEM consisting of 10% FBS and 100 U/mL penicillin-streptomycin for 24 h. After cell adherence, 0.01 µg/mL inductive DDP was added. After 15 to 20 days, cells were successively cultured with 0.04, 0.10, 0.40, 1.00, and 4.00 µg/mL DDP for 15 to 20 days each. Then, the stable drug-resistant cells U2OS/DDP were obtained. To sustain the drug resistance, cell lines were cultured with 4.00 µg/mL concentration for the duration of the study.

Experimental groups and cell transfection

MG63 cells were assigned into a control group, a negative control group (NC) (cells were transfected with NC plasmid of silenced lncRNA MSC-AS1), and a small interference (si)-MSC-AS1 group (cells were transfected with siRNA plasmid of lncRNA MSC-AS1). U2OS cells were assigned into a control group, a NC group (cells were transfected with NC plasmid of overexpressed lncRNA MSC-AS1), and an MSC-AS1 group (cells were transfected with overexpressed plasmid of lncRNA MSC-AS1).

U2OS/DDP cells were assigned into a control group, a NC group (cells were transfected with NC plasmid of silenced lncRNA MSC-AS1), a si-MSC-AS1-1 group (cells were transfected with siRNA-1 plasmid of lncRNA MSC-AS1), and a si-MSC-AS1-2 group (cells were transfected with siRNA-2 plasmid of lncRNA MSC-AS1).

Transfection was conducted using Lipofectamine 2000 (Invitrogen, Carlsbad, CA, USA) strictly following the manufacturer's instructions. Reverse transcription-quantitative polymerase chain reaction (RT-qPCR) was performed to verify transfection results 48 h later. The successfully transfected cells were saved for further experiments.

3-(4, 5-dimethylthiazol-2-yl)-2, 5-diphenyltetrazolium bromide (MTT) assay

OS cells in logarithmic growth phase from each group diluted to 1×10^4 cells/mL were cultured in 96-well plates, with 20 μ L prepared MTT solution added in each well. After 4 h, 150 μ L dimethyl sulfoxide (DMSO) was also added. The absorbance value was measured after 12, 24, 48, and 72 h, respectively, at 570 nm wavelength. Cell viability (%) was calculated by the equation $(OD_{\text{drug treated group}} - OD_{\text{control group}}) / (OD_{\text{control group}} - OD_{\text{vehicle group}})$ [17].

Colony formation assay

OS cells in exponential phase from each group were used to prepare a single-cell suspension. Then, 150 μ L cell suspension was inoculated into 6-well plates. When the colony formation was visible, 3 mL methanol was added in each well for a 15-min fixation, and Giemsa staining solution was added for 20 min to count colonies.

5-ethynyl-2'-deoxyuridine (EdU) assay

We inoculated 5×10^3 differentially treated OS cells in logarithmic growth phase in a 96-well plate with EdU dye (Wuhan RiboBio Biotech Co., Wuhan, China) for 2 h. The 4% paraformaldehyde-fixed cells were cultured for 30 h. Then, 100 μ L penetrant (phosphate-buffered saline [PBS] containing 0.5% TritonX-100) was added to perform incubation for 10 min. Cells stained by 1 \times Apollo[®] staining solution were incubated in the dark for 30 min. Finally, cells were stained with 25 μ g/mL Hoechst 33334 dye for 30 min without light exposure. After the staining, cell images were observed and captured under an inverted fluorescence microscope (OLYMPUS, Tokyo, Japan). EdU-positive cell rates were calculated and statistically analyzed.

Transwell assay

Matrigel diluted by 80 μ L DMEM at the ratio of 1: 6 was added to the chamber membrane and placed in a 37°C incubator for 2 h. OS cells in exponential phase were prepared for single-cell suspension. Differentially treated cells with the adjusted 2×10^5 cells/mL concentration were inoculated into a 96-well plate, with 500 μ L medium consisting of 10% serum, for 24 h. Chambers were fixed by 800 μ L methanol for 30 min and then stained by 800 μ L Giemsa staining solution for 15

to 30 min at room temperature. After soaking in clean water, the chamber was taken out, dried, and sealed for observation under the microscope.

Scratch test

Cells from each group were inoculated onto 6-well plates. After that, a pipette tip was used to draw a straight line perpendicular to the center on the cell surface after cells reached 100% confluence. The scratch was observed and photographed under the microscope after 0 h and 24 h. The rate of relative cell mobility was calculated as $(0 \text{ h scratch width} - 24 \text{ h scratch width}) / 0 \text{ h scratch width} \times 100\%$. Image analysis software was used to measure the scratch width 3 times to get the average value.

Flow cytometry

Differentially treated cells in exponential phase were prepared for single-cell suspension and centrifuged at 111 g for 5 min. Cells were incubated with Annexin V-FITC and propidium iodine (PI) in buffer solution for 15 min in the dark. Then, cells were centrifuged at 111 g for 5 min again to precipitate. After that, cells were cultured with fluorescence solution at 4°C for 20 min in the dark. Cell apoptosis rates were determined by flow cytometry.

RT-qPCR

Cells from each group were inoculated in an incubator at 1×10^4 cells/cm² and collected when cells reached 90% confluence. Trizol (Invitrogen) was applied to extract the total RNA from cells in exponential phase, and the concentration and purity of RNA was detected. Complementary DNA (cDNA) was synthesized using the RT kit and extended by a PCR apparatus. The primer sequences in Table 1 were determined using a SYBR PCR Master Mix kit. U6 served as the internal reference of miR-142, and β -actin served as the internal reference of lncRNA MSC-AS1 and CDK6. All the primers in the experiment were designed by the Primer 3Plus website, and synthesized by Genewiz, Inc. (Suzhou, Jiangsu, China). The experiments were performed 3 times to get the average value. Finally, RNA expression in cells and tissues were verified by the concentration of every sample according to the $2^{-\Delta\Delta CT}$ method.

Western blot analysis

Glyceraldehyde-3-phosphate dehydrogenase (GAPDH) served as an internal reference. According to the varied cell concentration in each group, cells were mixed with heated sodium dodecyl sulfonate (SDS) loading buffer for 5 min. After the electrophoresis separation conducted by sodium dodecyl sulfate polyacrylamide gel electrophoresis, 10 μ g proteins were

Table 1. Primers sequence.

Primer	Sequence (5'-3')
LncRNA MSC-AS1	Forward primer TCAAGAAATGGTGGCTAT
	Reverse primer GCTCTGAGACTGGCTGAA
miR-142	Forward primer TGTAGTGTTCCTACTTTATCCA
	Reverse primer CATAAAGTAGAAAGCACTACT
U6	Forward primer GCTTCGGCAGCACATACTAAAAT
	Reverse primer CGCTTCACGAATTGCGTGCAT
CDK6	Forward primer TGCACAGTGTCCAGAACAG
	Reverse primer ACCTCGGAGAAGCTGAAACA
β-actin	Forward primer GTCATTCCAAATATGAGAGATGCGT
	Reverse primer GCTATCACCTCCCCTGTGTG

LncRNA – long non-coding RNA; MSC – mesenchymal stem cell; miR – microRNA; CDK6 – cyclin-dependent kinase 6.

transferred into the polyvinylidene fluoride (PVDF) membranes. Membranes were cultivated with primary antibodies (Table 2) overnight and then were rinsed. Next, cells were cultured with secondary antibody (1/2000, ab67154) labeled by horseradish peroxidase (HRP) for 1 h. After full rinsing, cells were visualized by a fluorescent kit and recorded after X-ray exposure. The gray value in every stripe was scanned.

Nucleoplasmic separation and RNA extraction

After detachment, OS cells were centrifuged at low speed, mixed with 500 μL precooling fraction buffer, and centrifuged again after full pyrolysis in an ice-water bath for 5 to 10 min. The cytoplasmic component was extracted by supernatant and the nuclear component was extracted by precipitate. With 500 μL disruption buffer added, the precipitate was placed in the ice-water bath to reach complete dissolution. Cytoplasmic and nuclear component were mixed with 500 μL lysis buffer solution and 500 μL absolute ethyl alcohol, respectively, and recovered with a recovery column and stored at –80°C. The experiment was performed according to the instructions of the nucleoplasmic separation kit (Life Technologies, Rockford, IL, USA).

Dual-luciferase reporter gene assay

LncRNA MSC-AS1 and CDK6 3'UTR sequences consisting of miR-142 binding were synthesized to establish wild-type (WT) plasmids and mutant-type (MUT) plasmids of LncRNA MSC-AS1 and CDK6 3'UTR. After treatment, the WT and MUT plasmids were mixed with plasmids of NC and miR-142 to co-transfect into 293T cells (ATCC, USA). The collected cells were lysed 48 h later. Luciferase activity was detected using a luciferase detection kit (BioVision, San Francisco, CA, USA) and a Glomax20/20 luminometer (MPC12ison, Promega, WI, USA).

Table 2. Antibodies used in experiment.

Antibody	Information	Dilution rate
E-cadherin	ab40772,ABcam	1/10000
Vimentin	ab8978,ABcam	1/500
CDK6	ab151247,ABcam	1/500
p-PI3k	ab151549,ABcam	1/1000
t-PI3k	ab32089,ABcam	1/1000
p-AKT	ab38449,ABcam	1/1000
t-AKT	ab8805,ABcam	1/1000
GAPDH	ab181602,ABcam	1/10000

CDK6 – cyclin-dependent kinase 6; PI3K – phosphatidylinositol 3-kinase; GAPDH – glyceraldehyde-3-phosphate dehydrogenase.

RNA pull-down assay

Bio-miR-142-WT, Bio-miR142-MUT, and NC substance formed in OS cells were treated as the requirements of pull-down assay as described previously [18].

Xenograft tumors in nude mice

Eighteen specific pathogen-free (SPF) male BALB/c nude mice (4 to 6 weeks old, weight 16 to 18 g) (Vital River Animal Co., Zhejiang, China) were divided into a control group, a NC group (with NC plasmid of silenced LncRNA MSC-AS1), and a MSC-AS1 group (with siRNA plasmid of LncRNA MSC-AS1). The plasmids were injected subcutaneously into corresponding nude mice, and tumor volume (mm³) was determined using the formula $V=L \times W^2 \times 0.5$ every 3 days, with a growth curve drawn. On the 21st day, mice were sacrificed by cervical dislocation. After that, the skin was cut off to separate and weigh the tumors for the following procedures.

Immunocytochemistry staining

Ki67 (5 μg/mL, ab15580) expression was determined in accordance with the instructions of the immunohistochemical streptavidin-peroxidase (SP) kit (Zhongshan Golden Bridge Biotech Co., Beijing, China).

Statistical analysis

SPSS 21.0 (IBM Corp. Armonk, NY, USA) was used for data analysis. The Kolmogorov-Smirnov test results indicated whether the data were in normal distribution. The results were shown in mean ± standard deviation. Kaplan-Meier assay was applied for analyzing survival rates. The *t* test was used for analysis of

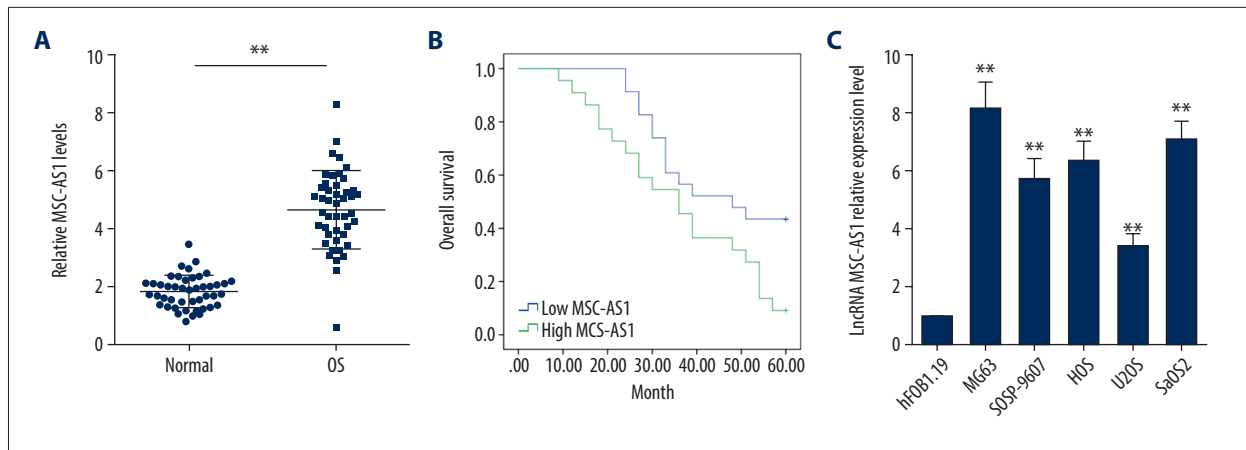


Figure 1. lncRNA MSC-AS1 is upregulated in OS and is associated with poor prognosis. (A) RT-qPCR results showed that lncRNA MSC-AS1 expression was significantly higher in OS tissues than in adjacent normal bone tissues, $n=45$. (B) Relationship between lncRNA MSC-AS1 expression and prognosis of OS patients was analyzed by Kaplan-Meier assay, $n=45$. (C) lncRNA MSC-AS1 expression in human normal osteoblast hFOB1.19 cells and OS cell lines were detected by RT-qPCR. The experiments were performed 3 times; compared with normal group/hFOB1.19 cells, $** p<0.05$. The independent-samples t test was used for statistical analysis of comparisons in (A), Kaplan-Meier assay was utilized to analyze (B), and one-way ANOVA and Tukey's multiple comparisons test were applied to determine (C). lncRNA – long non-coding RNA; OS – osteosarcoma; RT-qPCR – reverse transcription-quantitative polymerase chain reaction; ANOVA – analysis of variance.

comparisons between 2 groups, one-way or two-way analysis of variance (ANOVA) was used for comparisons among multiple groups, and Tukey's multiple comparisons test/Sidak's multiple comparisons test was used for pairwise comparisons after ANOVA. The p value was attained using a two-tailed test and $p<0.05$ regarded as indicating a significant difference.

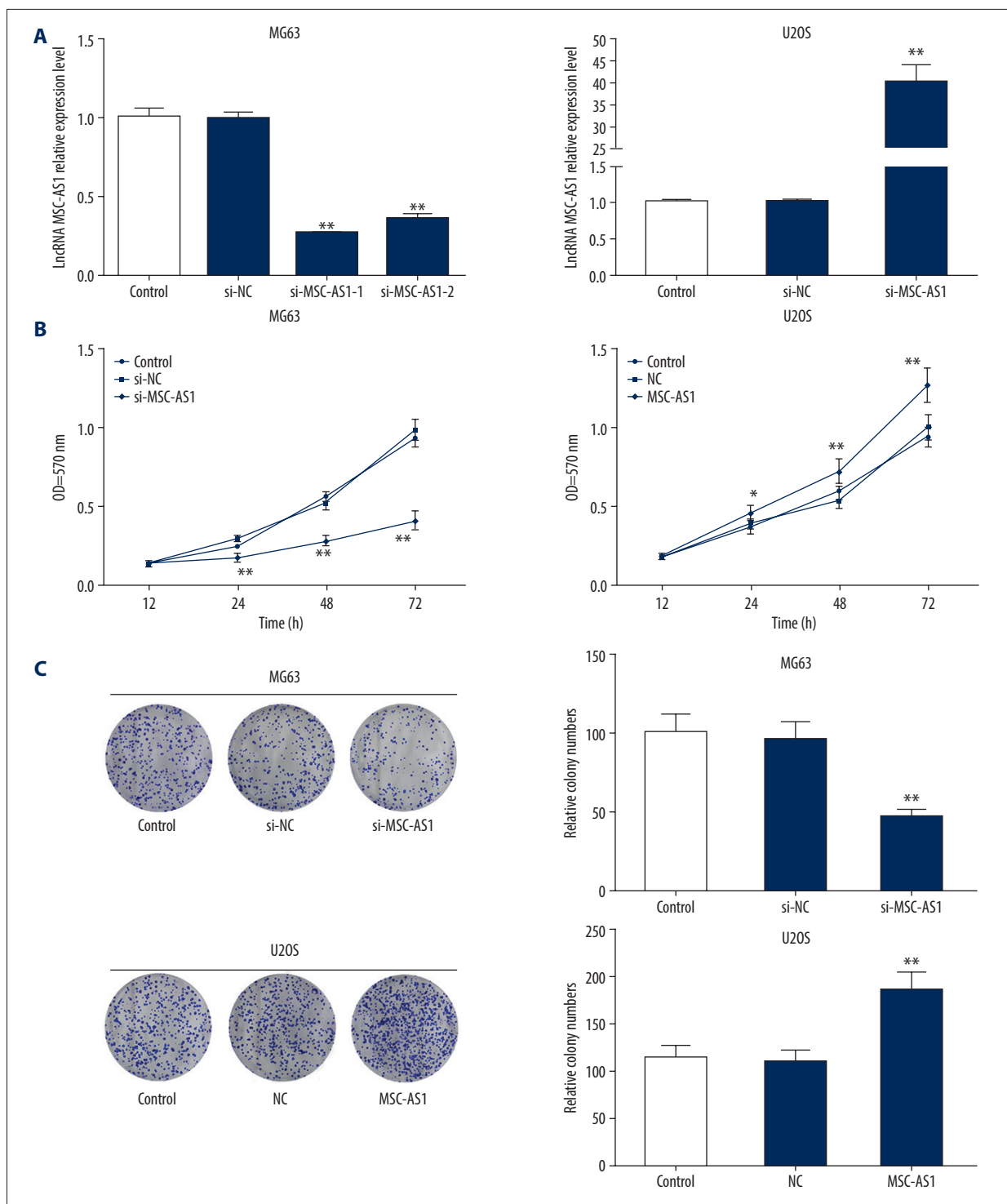
Results

Upregulated lncRNA MSC-AS1 in OS leads to poor prognosis

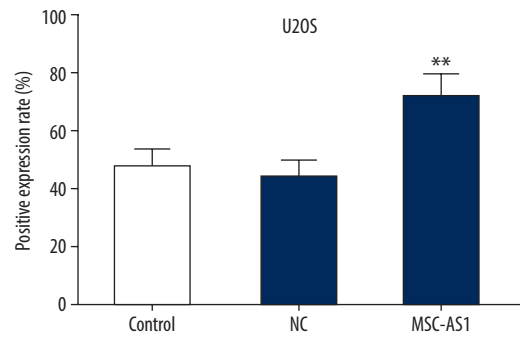
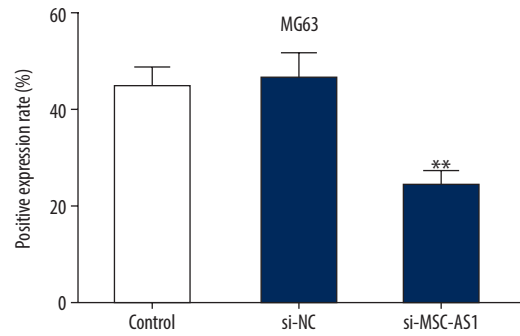
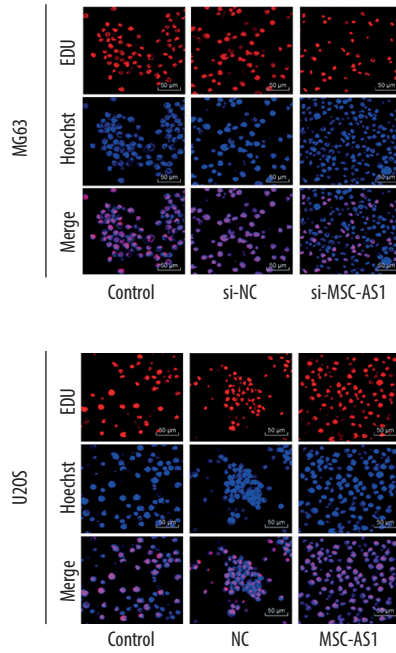
lncRNA MSC-AS1 expression in the 45 OS tissues and adjacent normal bone tissues were assessed. It was discovered that lncRNA MSC-AS1 expression was evidently higher in OS tissues than in adjacent normal bone tissues ($p<0.05$). According to median of lncRNA MSC-AS1 expression, the 45 patients were divided into a poorly-expressed group ($n=23$) and a highly-expressed group ($n=22$). We found that highly expressed lncRNA MSC-AS1 was related to poor prognosis of OS patients. Assessment of lncRNA MSC-AS1 expression in human normal osteoblast hFOB1.19 cells and OS cell lines showed that MG63, SOSP-9607, HOS, U2OS, and lncRNA MSC-AS1 expression in OS cell lines was significantly higher than in hFOB1.19 cells (Figure 1A–1C).

Silenced lncRNA MSC-AS1 inhibits OS cell progression and epithelial-mesenchymal transition (EMT) and promotes OS cell apoptosis

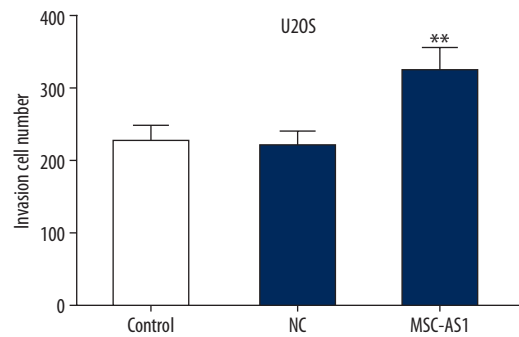
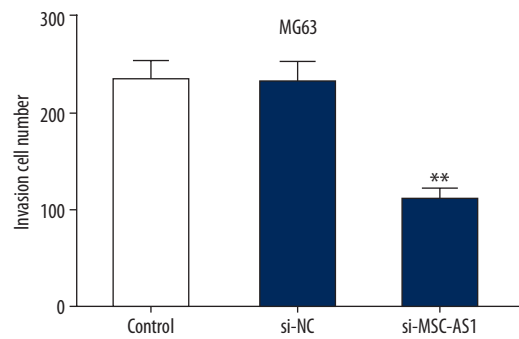
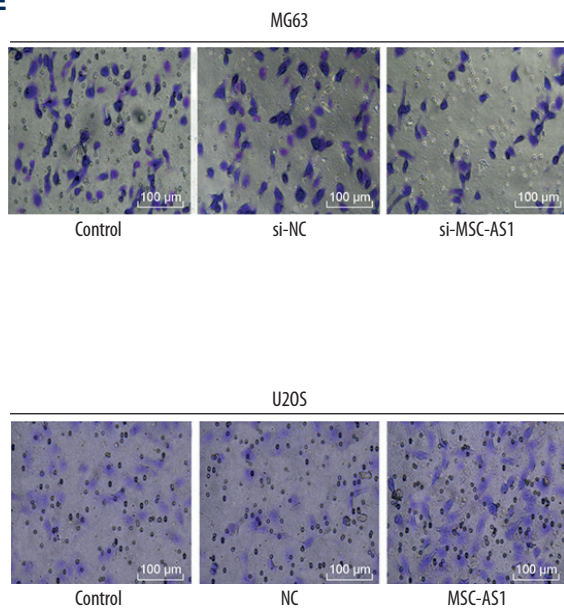
lncRNA MSC-AS1 expression was upregulated in U2OS cells, providing insights into the mechanism of lncRNA MSC-AS1 in OS progression. The constructed overexpressed plasmids of lncRNA MSC-AS1 were transfected into U2OS cells, while the plasmids of lncRNA MSC-AS1 siRNAs were transfected into MG63 cells. The results from RT-qPCR showed successful transfections, and lncRNA MSC-AS1-1 was more completely transfected than lncRNA MSC-AS1-2; therefore, we selected lncRNA MSC-AS1-1 for further experimentation (Figure 2A). Cell proliferation was detected using MTT, colony formation assay, and EdU assay. The results suggested that OS cell viability, the number of colonies, EdU-positive cells, and cell invasion and migration were significantly decreased in cells with poorly expressed lncRNA MSC-AS1 (all $p<0.05$). On the contrary, all the indices mentioned above in U2OS cells with highly expressed lncRNA MSC-AS1 were quite opposite (Figure 2A–2F). Additionally, poorly expressed lncRNA MSC-AS1 brought about a huge increase in E-cadherin expression and a great decrease in vimentin expression (both $p<0.05$). However, highly expressed lncRNA MSC-AS1 resulted in the opposite outcomes (Figure 2G). We also found that cell apoptosis was promoted as lncRNA MSC-AS1 expression was suppressed and was reduced in overexpressed lncRNA MSC-AS1 ($p<0.05$) (Figure 2H).



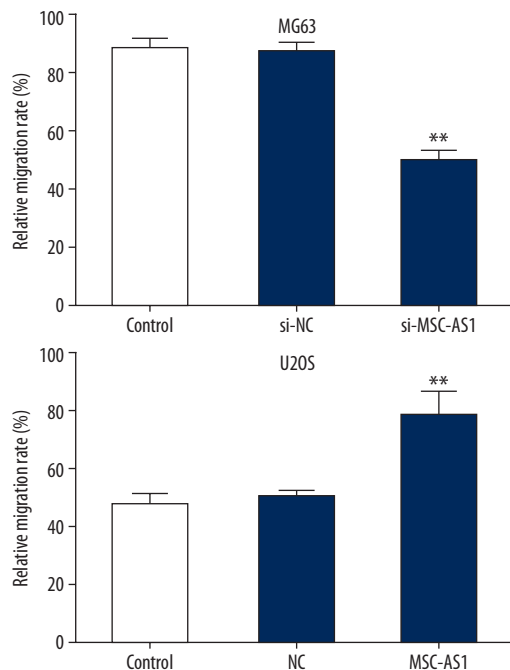
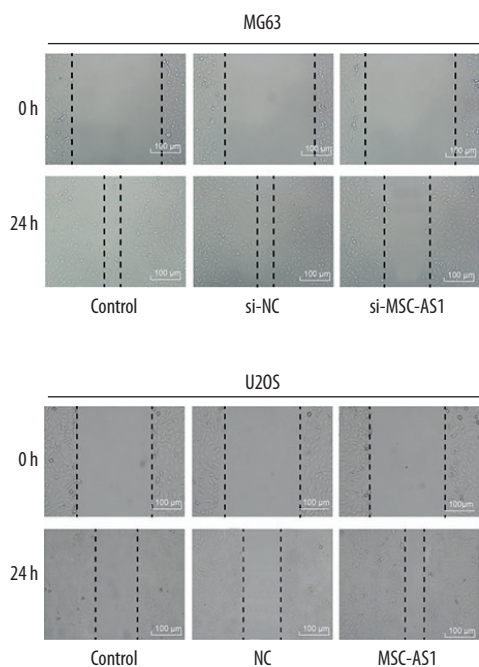
D



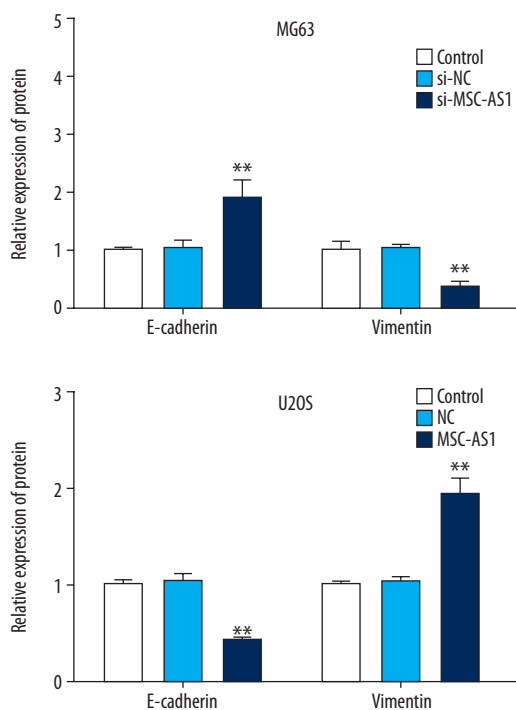
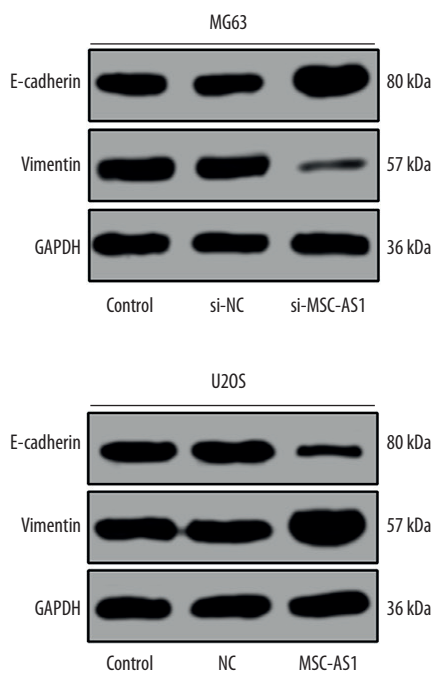
E



F



G



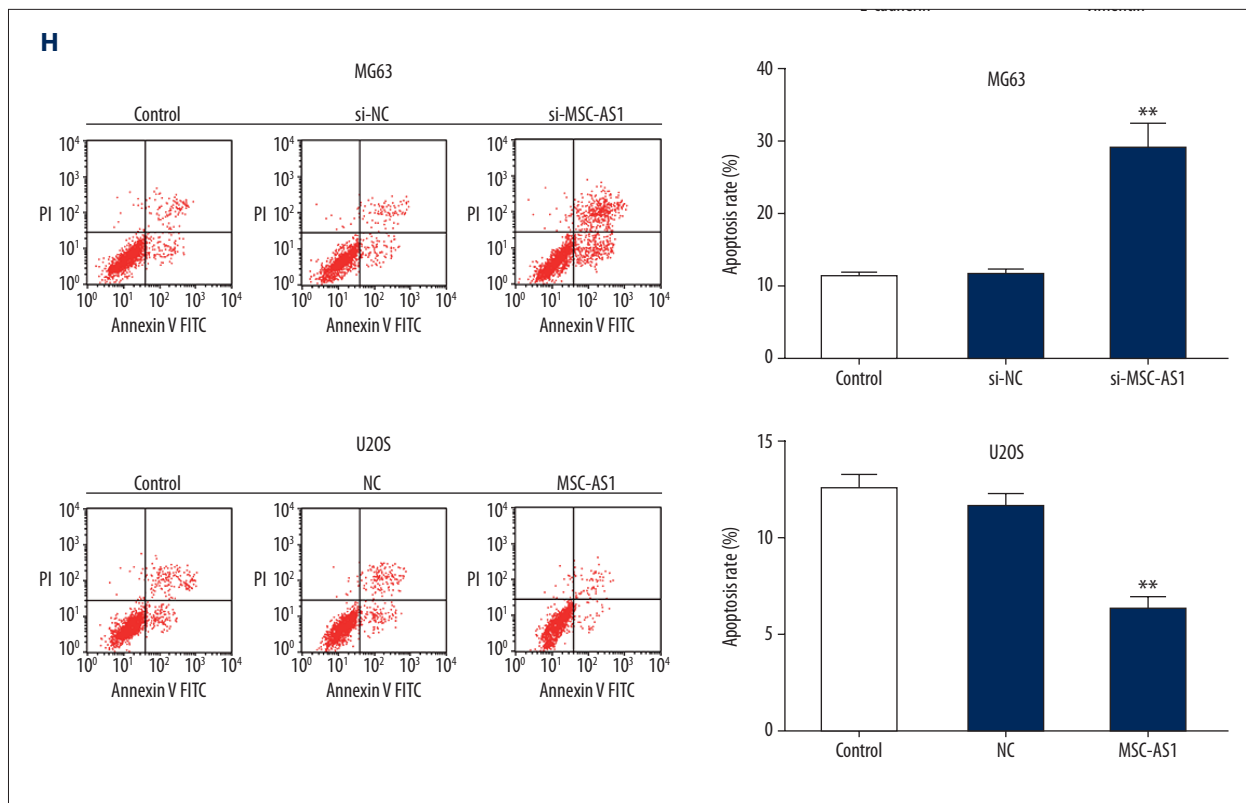


Figure 2. Silencing of lncRNA MSC-AS1 reduced OS cell proliferation, invasion, migration and EMT and increased OS cell apoptosis. (A) lncRNA MSC-AS1 expression in transfected OS cells MG63 and U2OS was assessed with RT-qPCR. (B) OS cell viability in all groups was detected by MTT assay. (C) Colony formation ability in OS cells from all groups was measured. (D) DNA replication in all groups was detected by EdU assay. (E) OS cell invasion in all groups was assessed with Transwell assay. (F) OS cell migration in all groups was verified by scratch test. (G) EMT-related protein expression in all groups was measured by Western blot analysis. (H) OS cell apoptosis in all groups was assessed with flow cytometry. Compared with control group, * $p < 0.05$, ** $p < 0.01$. The experiments were performed 3 times; one-way ANOVA and Tukey's multiple comparisons test were applied to determine (A, C–F, H), and two-way ANOVA and Tukey's multiple comparisons test were applied to determine (B, G). lncRNA – long non-coding RNA; EMT – epithelial-mesenchymal transition; OS – osteosarcoma; RT-qPCR – reverse transcription-quantitative polymerase chain reaction; MTT – 3-(4, 5-dimethylthiazol-2-yl)-2, 5-diphenyltetrazolium bromide; EdU – 5-ethynyl-2'-deoxyuridine; ANOVA – analysis of variance.

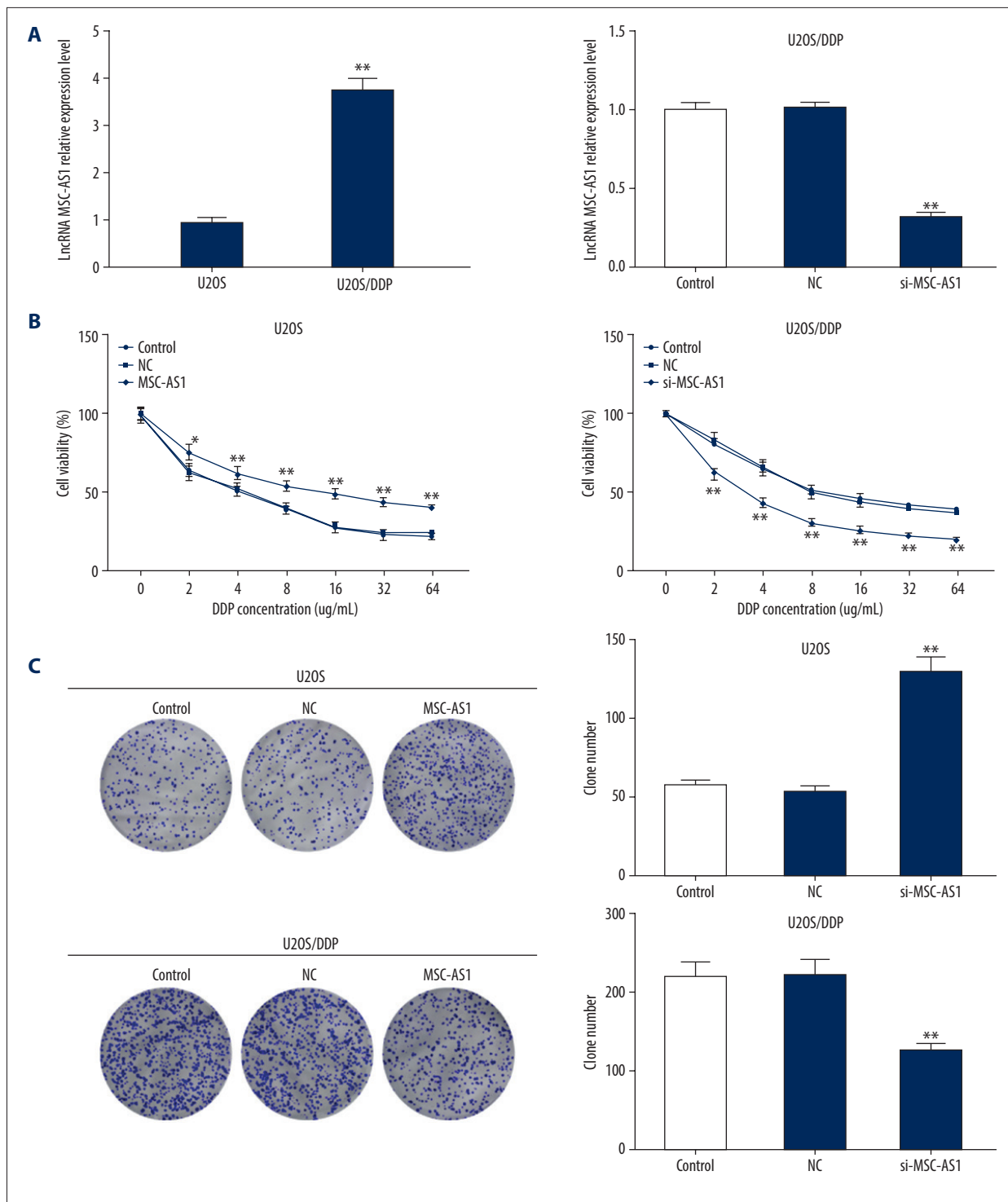
Silenced lncRNA MSC-AS1 makes OS cells more sensitive to DDP

Effects of lncRNA MSC-AS1 on OS cell susceptibility to DDP were further assessed. Our experiments showed that lncRNA MSC-AS1 expression was evidently higher in U2OS/DDP cells than in U2OS cells, while it was downregulated when U2OS/DDP cells were transfected with si-MSC-AS1 (Figure 3A). Various concentrations of DDP were subjected to transfected U2OS cells and U2OS/DDP cells, and it was found that cell viability was reduced when the DDP concentration increased. U2OS cell survival rates were around 50% in the 4 $\mu\text{g}/\text{mL}$ DDP group, and U2OS/DDP cell survival rates were around 50% in the 8 $\mu\text{g}/\text{mL}$ DDP group. Therefore, 4 $\mu\text{g}/\text{mL}$ DDP was selected for U2OS cell treatment and 8 $\mu\text{g}/\text{mL}$ DDP was selected for U2OS/DDP cell treatment in further experiments.

Colony formation assay and flow cytometry showed that low lncRNA MSC-AS1 expression strengthened OS cell sensitivity to DDP, while overexpressed lncRNA MSC-AS1 resulted in the opposite effect (Figure 3B–3D).

lncRNA MSC-AS1 competitively binds to miR-142, thereby elevating CDK6 and activating the PI3K/AKT signaling pathway

Because of the important role molecule location plays in biological function, we used a bioinformatics website (<http://lncatlas.crg.eu/>) and found that lncRNA MSC-AS1 was mainly localized in the cytoplasm (Figure 4A). Nucleoplasmic separation further confirmed that lncRNA MSC-AS1 was mainly found in cytoplasm (Figure 4B). A previous study discovered that, acting as a tumor suppressor in OS, miR-142 inhibited cell proliferation and invasion at S phase to delay



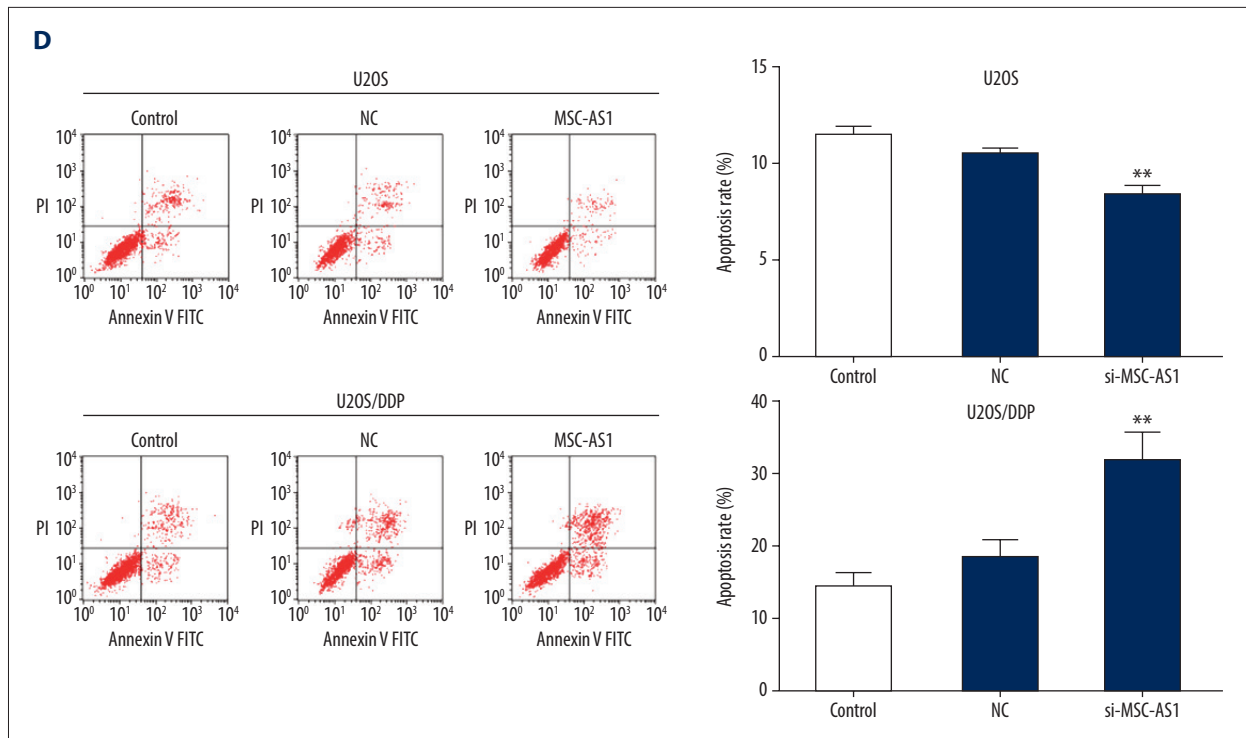


Figure 3. Silencing of lncRNA MSC-AS1 makes OS cells more sensitive to cisplatin. (A) lncRNA MSC-AS1 expression in transfected U2OS cells and U2OS/DDP cells was detected by RT-qPCR. (B) U2OS and U2OS/DDP cell viabilities in different DDP concentrations (0, 2, 4, 8, 16, 32, 64 $\mu\text{g/mL}$) were measured by MTT assay. (C) U2OS cell colony formation ability treated by 4 $\mu\text{g/mL}$ DDP and U2OS/DDP cell colony formation ability treated by 8 $\mu\text{g/mL}$ DDP were assessed by colony formation assay. (D) U2OS cell apoptosis treated with 4 $\mu\text{g/mL}$ DDP and U2OS/DDP cell apoptosis treated with 8 $\mu\text{g/mL}$ DDP was detected by flow cytometry. Compared with control group, * $p < 0.05$, ** $p < 0.01$, the experiments were performed 3 times, one-way ANOVA and the t test were applied to determine (A, C, D), and two-way ANOVA and Tukey's multiple comparisons test were applied to determine (B). lncRNA – long non-coding RNA; OS – osteosarcoma; RT-qPCR – reverse transcription-quantitative polymerase chain reaction; MTT – 3-(4, 5-dimethylthiazol-2-yl)-2, 5-diphenyltetrazolium bromide; ANOVA – analysis of variance.

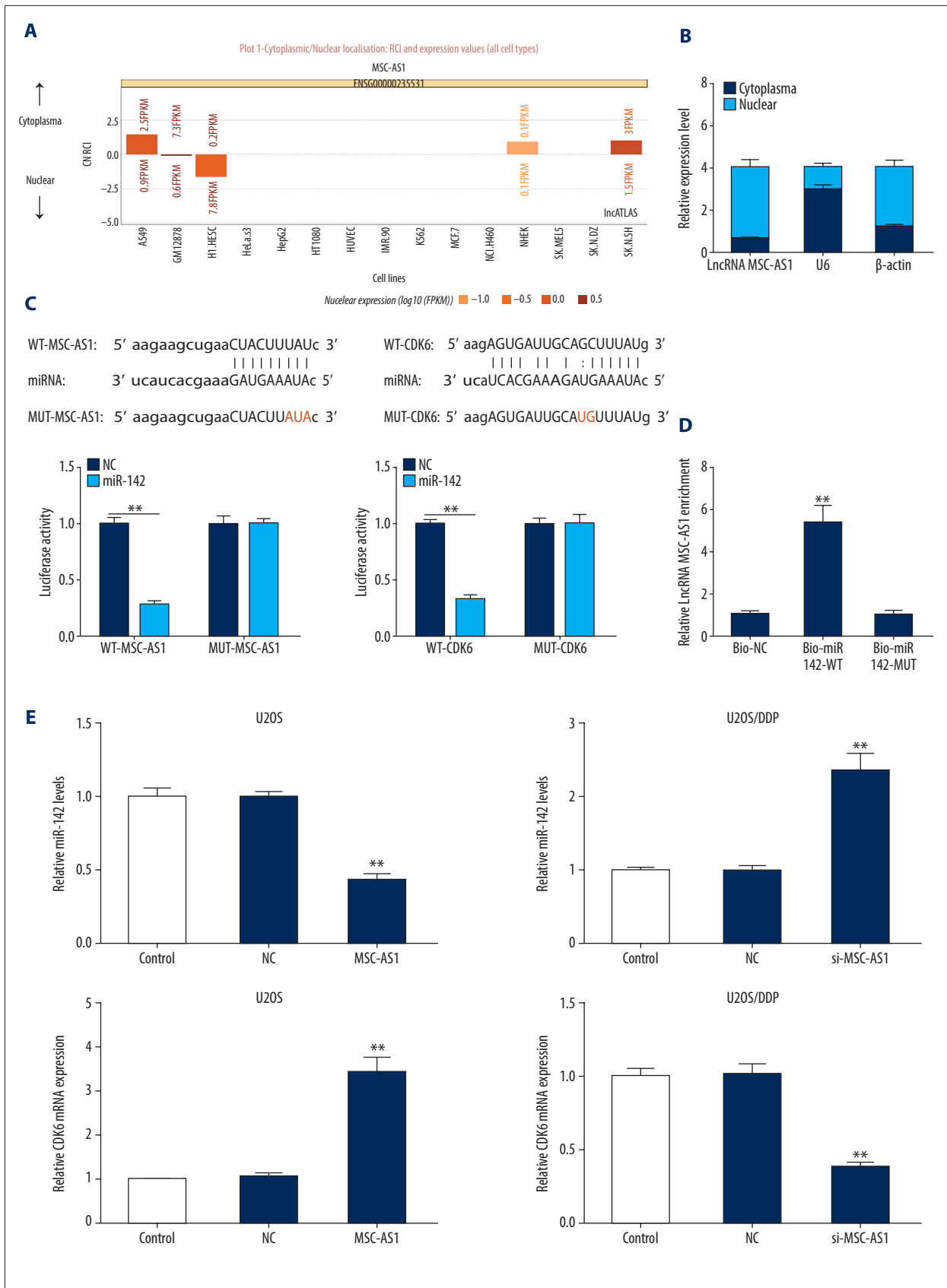
the cell cycle. Moreover, miR-142 inhibited OS cell invasion by inducing E-cadherin expression and reducing expression of matrix metalloproteinase 2 (MMP2) and MMP9 [19]. It was reported that downregulation of miR-142 was observed in OS cells, and miR-494 restrained OS cell progression by targeting CDK6 [20]. Using the bioinformatics website (<http://starbase.sysu.edu.cn/index.php>), we found that both lncRNA MSC-AS1 and CDK6 were combined to miR-142 at some sites. The findings of dual-luciferase reporter gene assay showed decreased luciferase activity of WT lncRNA MSC-AS1 and miR-142, and that of WT CDK6 and miR-142 also significantly declined (both $p < 0.05$) (Figure 4C). RNA pull-down assay provided another confirmation that there was a binding site between lncRNA MSC-AS1 and miR-142 (Figure 4D). With lncRNA MSC-AS1 knockdown, miR-142 was significantly elevated, while mRNA and protein expression in CDK6 was greatly decreased, and protein expression in p-PI3K/t-PI3K and p-AKT/t-AKT also steeply declined (all $p < 0.05$), but all these results were the opposite with overexpressed lncRNA MSC-AS1 (Figure 4E, 4F).

Silenced lncRNA MSC-AS1 inhibits OS cell *in vivo*

To determine the effects of lncRNA MSC-AS1 on OS cell oncogenesis *in vivo*, MG63 cells were subcutaneously injected into nude mice, and the tumors were weighed every 3 days. It was found that tumor volume in differentially treated mice increased over time. Tumor volume and weight declined in mice with poorly expressed lncRNA MSC-AS1 ($p < 0.05$) (Figure 5A, 5B). Finally, results from immunocytochemistry showed that the Ki67-positive expression rate was significantly suppressed in mice with poorly expressed lncRNA MSC-AS1 ($p < 0.05$) (Figure 5C).

Discussion

Consisting of osteoid-generating spindle cells, highly aggressive and malignant OS is a common primary bone tumor occurring in the skeletal system [21]. As a key oncogene or suppressor found in tumor growth, lncRNAs are independent markers and targets in cancer detection, treatment, and



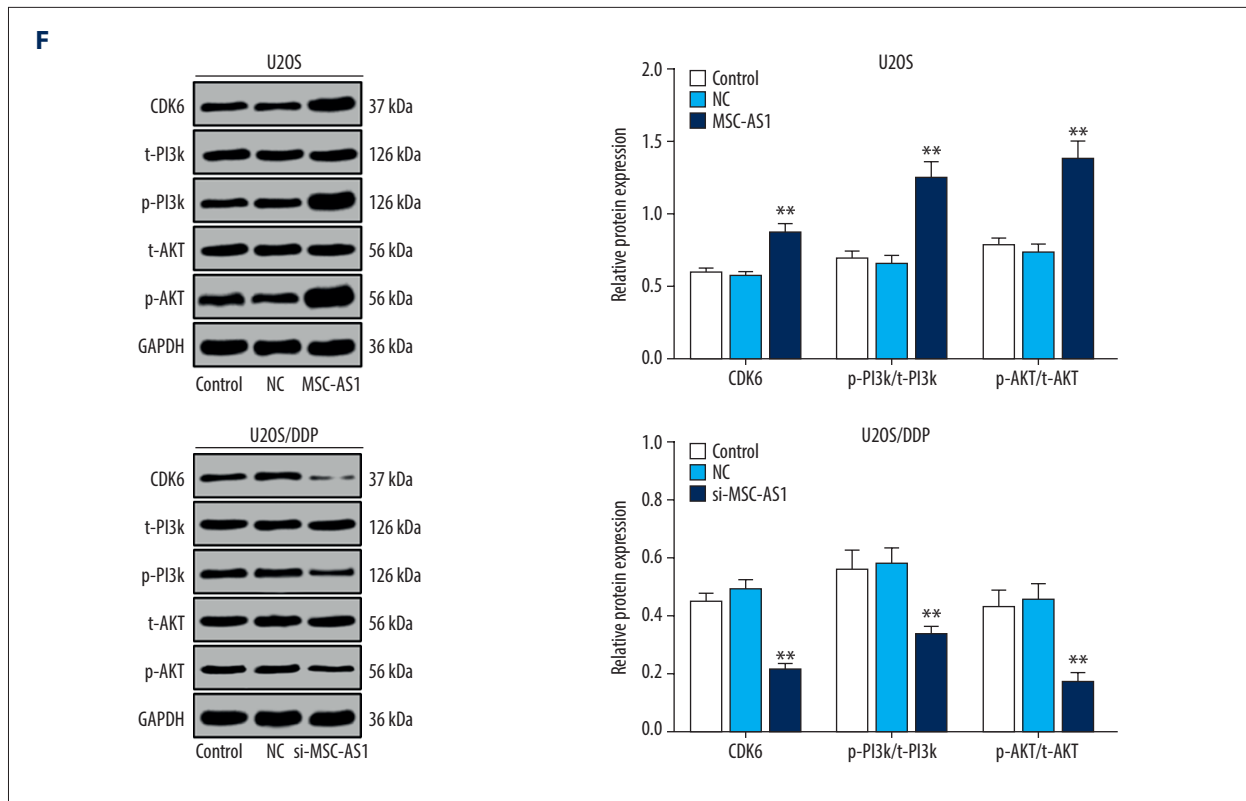


Figure 4. lncRNA MSC-AS1 binds to miR-142, thereby reducing miR-142-targeted inhibition of CDK6 and modulating PI3K/AKT signaling pathway activation. (A) A bioinformatics website was used to determine that lncRNA MSC-AS1 was mainly localized in the cytoplasm. (B) Nucleoplasmic separation assay indicated that lncRNA MSC-AS1 was mainly found in cytoplasm. (C) The bioinformatics website and dual-luciferase reporter gene assay helped to discover that both lncRNA MSC-AS1 and CDK6 were combined to miR-142 at some sites. (D) RNA pull-down assay showed the adsorptive effect of lncRNA MSC-AS1 on miR-142. (E) miR-142 expression in U2OS cells and U2OS/DDP cells, as well as mRNA expression of CDK6, were measured by RT-qPCR. (F) CDK6, p-PI3K, t-PI3K, p-AKT, and t-AKT expression in U2OS cells and U2OS/DDP cells were verified with Western blot analysis. Compared with the control group, ** $p < 0.01$, the experiments were performed 3 times, one-way ANOVA and Tukey's multiple comparisons test were applied to determine (D, E); two-way ANOVA and Tukey's multiple comparisons test were applied to determine (B, F), two-way ANOVA and Sidak's multiple comparisons test were applied to determine (C). lncRNA – long non-coding RNA; miR – microRNA; CDK6 – cyclin-dependent kinase 6; PI3K – phosphatidylinositol 3-kinase; RT-qPCR – reverse transcription-quantitative polymerase chain reaction; ANOVA – analysis of variance.

prognosis by deregulating OS cell pathogenesis [22]. A previous study suggested that overexpressed MSC-AS1 is highly associated with PDAC cells with distant metastasis and advanced tumor lymph node metastasis [10]. miRs are already regarded as a standard in assessment in cancer clinics by affecting different oncogenes and tumor suppressor genes expression [23]. Gain-of-function assays indicated that miR-142 overexpression reduced OS cell development by suppressing cell proliferation and invasion and arrested the cell cycle in the S phase [19]. In the present study, we assessed the mechanism of lncRNA MSC-AS1 in OS biological behaviors and cell sensitivity to DDP via binding to miR-142. Consequently, our data showed that downregulated MSC-AS1 could promote expression of miR-142 to decrease CDK6 expression and inhibit the activation of the PI3K/AKT signaling pathway to slow OS progression and make it more sensitive to DDP.

We showed that upregulated MSC-AS1 predicted a poor prognosis of OS patients. A prior study has suggested that MSC-AS1 is highly expressed in PDAC cells and tissues [10]. Another study has demonstrated that MSC-AS1 is closely associated with recurrence-free survival in hepatocellular carcinoma [24]. Our study also suggests that OS cell progression and EMT were slowed and cell apoptosis was enhanced after silencing MSC-AS1. As a vascular endothelial cell transition induced by transcription factors that adjust gene expression to reduce cell-cell adhesion, EMT is actively involved in progression of many cancer [25]. Our functional assays found that the EMT-related protein E-cadherin was noticeably enhanced and vimentin was steeply decreased after silencing MSC-AS1. High expression of E-cadherin brought about a loss of function in cancer cells and is associated with improved survival rates and prognosis in many kinds of cancers [26]. Vimentin is associated with

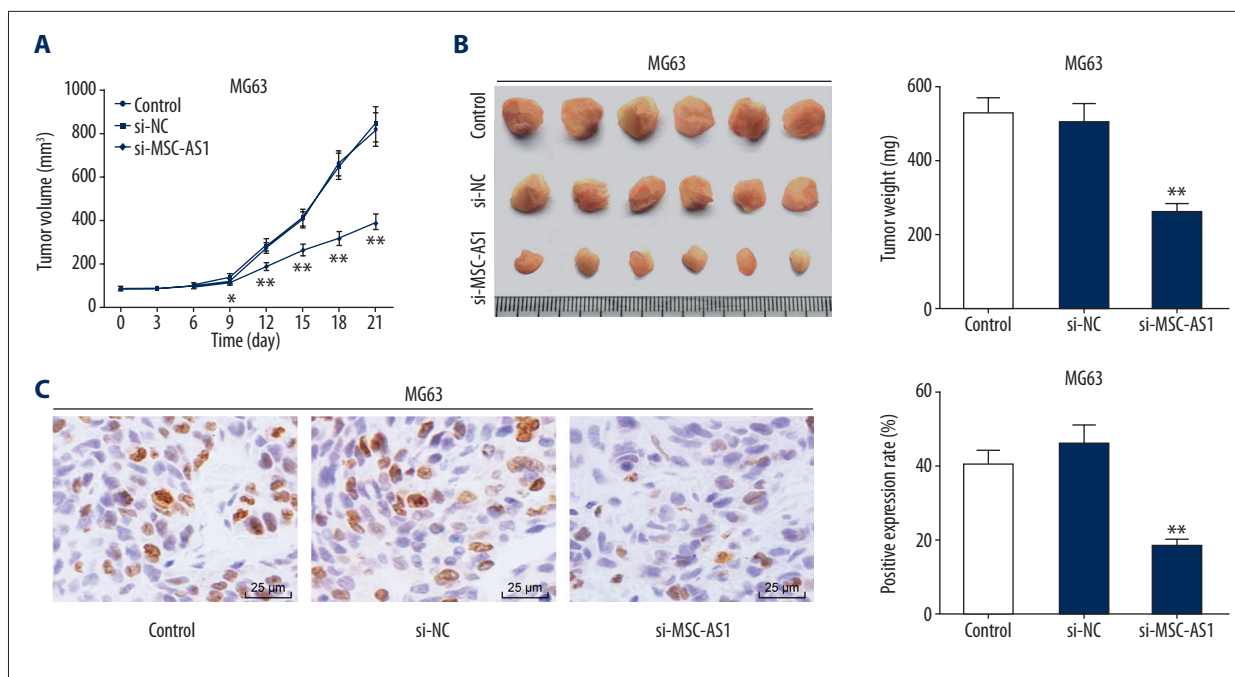


Figure 5. Silenced lncRNA MSC-AS1 inhibits OS cell *in vivo*. (A) Tumor volumes in all groups were calculated every 3 days using the formula $V=L \times W^2 \times 0.5$. (B) On the 21st day, the tumors were taken out and weighed. (C) Ki67-positive expression of tumors in each group was detected by immunohistochemistry. N=6 in each group, compared with the control group, * $p < 0.05$, ** $p < 0.01$. Two-way ANOVA and Tukey's multiple comparisons test were applied to determine (A), and one-way ANOVA and Tukey's multiple comparisons test were applied to determine (B, C). lncRNA – long non-coding RNA; OS – osteosarcoma; ANOVA – analysis of variance.

actively aggressive tumor phenotypes and metastasis progression in canine bone tumors [27]. Cell apoptosis is an important part of OS treatment and it can effectively eliminate some OS cells [28]. In the present study, we performed a series of experiments to assess OS cell sensitivity to DDP with downregulated MSC-AS1. DDP, an effective chemotherapeutic drug used to treat many human cancers, accelerates cell apoptosis by limiting the DNA repair function and damaging DNA [29]. Evidence has shown that the growing problem of DDP resistance greatly limits the effectiveness of OS treatment [30]. Silenced MSC-AS1 provides a positive and effective response in OS treatment.

Additionally, website prediction confirmed the adsorptive link between MSC-AS1 and miR-142, and miR-142-targeted inhibition of CDK6 was reduced and PI3K/AKT signaling pathway activation was downregulated by silencing MSC-AS1. It was previously reported that decreased miR-142 expression in OS growth led to aberrant exchanges of target genes of miR-142, suggesting that miR-142 plays a role in OS [31]. Inhibitors of CDK6 show promise in cancer treatment [32]. Yuan et al. conducted a series of assays to determine the targeted links between miR-494 and CKD6, finding that overexpressed miR-494 significantly reduced CDK6 expression [20]. The active molecular changes and activities of the PI3K/AKT signaling pathway

in various cancers make it a key factor affecting cell biological behaviors [33]. A previous study has revealed that upregulation of the PI3K/AKT signaling pathway increased OS progression by improving cell cycle processes and reducing cell apoptosis [34]. Finally, results from xenograft tumors in nude mice show that silencing of MSC-AS1 reduced OS cell growth *in vivo*. Likewise, highly expressed lncRNA EWSAT1, a widely recognized tumor promoter in many human cancers, was found to be significantly associated with poor prognosis [35]. The evidence presented above suggest that downregulation of MSC-AS1 can slow OS progression.

Conclusions

Our study shows that silencing of lncRNA MSC-AS1 inhibits OS development by binding to miR-142, decreasing CDK6, and downregulating the PI3K/AKT signaling pathway. These results suggest a feasible approach for OS therapy and may be helpful in finding reliable therapeutic targets for OS. Although the results of the present study have therapeutic implications regarding OS development, it is preclinical research, and the experimental results and effective application in clinical practice need validation in further research.

Availability of data and materials

All the data generated or analyzed during this study are included in this published article.

Conflict of interest

None.

References:

1. Biazzo A, De Paolis M: Multidisciplinary approach to osteosarcoma. *Acta Orthop Belg*, 2016; 82(4): 690–98
2. Namlos HM, Meza-Zepeda LA, Baroy T et al: Modulation of the osteosarcoma expression phenotype by microRNAs. *PLoS One*, 2012; 7(10): e48086
3. Savage SA, Mirabello L: Using epidemiology and genomics to understand osteosarcoma etiology. *Sarcoma*, 2011; 2011: 548151
4. Jia J, Tian Q, Liu Y et al: Interactive effect of bisphenol A (BPA) exposure with -22G/C polymorphism in LOX gene on the risk of osteosarcoma. *Asian Pac J Cancer Prev*, 2013; 14(6): 3805–8
5. Wolfe TD, Pillai SP, Hildreth BE 3rd et al: Effect of zoledronic acid and amputation on bone invasion and lung metastasis of canine osteosarcoma in nude mice. *Clin Exp Metastasis*, 2011; 28(4): 377–89
6. Simpson E, Brown HL: Understanding osteosarcomas. *JAAPA*, 2018; 31(8): 15–19
7. McGuire J, Utset-Ward TJ, Reed DR, Lynch CC: Re-calculating! Navigating through the osteosarcoma treatment roadblock. *Pharmacol Res*, 2017; 117: 54–64
8. Guo ZH, You ZH, Wang YB et al: A Learning-based method for LncRNA-disease association identification combining similarity information and rotation forest. *iScience*, 2019; 19: 786–95
9. Li Z, Dou P, Liu T, He S: Application of long noncoding RNAs in osteosarcoma: Biomarkers and therapeutic targets. *Cell Physiol Biochem*, 2017; 42(4): 1407–19
10. Sun Y, Wang P, Yang W et al: The role of lncRNA MSC-AS1/miR-29b-3p axis-mediated CDK14 modulation in pancreatic cancer proliferation and Gemcitabine-induced apoptosis. *Cancer Biol Ther*, 2019; 20(6): 729–39
11. Ram Kumar RM, Boro A, Fuchs B: Involvement and clinical aspects of microRNA in osteosarcoma. *Int J Mol Sci*, 2016; 17(6): pii: E877
12. Gao YF, Zhang QJ, Yu Z et al: miR-142 suppresses proliferation and induces apoptosis of osteosarcoma cells by upregulating Rb. *Oncol Lett*, 2018; 16(1): 733–40
13. Tigan AS, Bellutti F, Kollmann K et al: CDK6—a review of the past and a glimpse into the future: From cell-cycle control to transcriptional regulation. *Oncogene*, 2016; 35(24): 3083–91
14. Zhu K, Liu L, Zhang J et al: MiR-29b suppresses the proliferation and migration of osteosarcoma cells by targeting CDK6. *Protein Cell*, 2016; 7(6): 434–44
15. Aoki M, Fujishita T: Oncogenic roles of the PI3K/AKT/mTOR Axis. *Curr Top Microbiol Immunol*, 2017; 407: 153–89
16. Wang Y, Leng H, Chen H et al: Knockdown of UBE2T inhibits osteosarcoma cell proliferation, migration, and invasion by suppressing the PI3K/Akt signaling pathway. *Oncol Res*, 2016; 24(5): 361–69
17. Wang S, Meng Q, Xie Q, Zhang M: Effect and mechanism of resveratrol on drug resistance in human bladder cancer cells. *Mol Med Rep*, 2017; 15(3): 1179–87
18. Chen X, Gao J, Yu Y et al: LncRNA FOXD3-AS1 promotes proliferation, invasion and migration of cutaneous malignant melanoma via regulating miR-325/MAP3K2. *Biomed Pharmacother*, 2019; 120: 109438
19. Zheng Z, Ding M, Ni J et al: MiR-142 acts as a tumor suppressor in osteosarcoma cell lines by targeting Rac1. *Oncol Rep*, 2015; 33(3): 1291–99
20. Yuan W, Wang D, Liu Y et al: miR494 inhibits cell proliferation and metastasis via targeting of CDK6 in osteosarcoma. *Mol Med Rep*, 2017; 16(6): 8627–34
21. Mathkour M, Garces J, Beard B et al: Primary high-grade osteosarcoma of the clavus: A case report and literature review. *World Neurosurg*, 2016; 89: 730e9–13
22. Chen R, Wang G, Zheng Y et al: Long non-coding RNAs in osteosarcoma. *Oncotarget*, 2017; 8(12): 20462–75
23. Reddy KB: MicroRNA (miRNA) in cancer. *Cancer Cell Int*, 2015; 15: 38
24. Gu JX, Zhang X, Miao RC et al: Six-long non-coding RNA signature predicts recurrence-free survival in hepatocellular carcinoma. *World J Gastroenterol*, 2019; 25(2): 220–32
25. Gonzalez DM, Medici D: Signaling mechanisms of the epithelial-mesenchymal transition. *Sci Signal*, 2014; 7(344): re8
26. Wong SHM, Fang CM, Chuah LH et al: E-cadherin: Its dysregulation in carcinogenesis and clinical implications. *Crit Rev Oncol Hematol*, 2018; 121: 11–22
27. Amaral CB, Leite JDS, Fonseca ABM, Ferreira AMR: Vimentin, osteocalcin and osteonectin expression in canine primary bone tumors: Diagnostic and prognostic implications. *Mol Biol Rep*, 2018; 45(5): 1289–96
28. Li J, Yang Z, Li Y et al: Cell apoptosis, autophagy and necroptosis in osteosarcoma treatment. *Oncotarget*, 2016; 7(28): 44763–78
29. Dasari S, Tchounwou PB: Cisplatin in cancer therapy: Molecular mechanisms of action. *Eur J Pharmacol*, 2014; 740: 364–78
30. Song L, Duan P, Gan Y et al: Silencing LPAATbeta inhibits tumor growth of cisplatin-resistant human osteosarcoma *in vivo* and *in vitro*. *Int J Oncol*, 2017; 50(2): 535–44
31. Shabani P, Izadpanah S, Aghebati-Maleki A et al: Role of miR-142 in the pathogenesis of osteosarcoma and its potential as therapeutic approach. *J Cell Biochem*, 2019; 120(4): 4783–93
32. Wang H, Nicolay BN, Chick JM et al: The metabolic function of cyclin D3-CDK6 kinase in cancer cell survival. *Nature*, 2017; 546(7658): 426–30
33. Sathe A, Nawroth R: Targeting the PI3K/AKT/mTOR pathway in bladder cancer. *Methods Mol Biol*, 2018; 1655: 335–50
34. Zhang J, Yu XH, Yan YG et al: PI3K/Akt signaling in osteosarcoma. *Clin Chim Acta*, 2015; 444: 182–92
35. Zhang GY, Zhang JF, Hu XM et al: Clinical significance of long non-coding RNA EWSAT1 as a novel prognostic biomarker in osteosarcoma. *Eur Rev Med Pharmacol Sci*, 2017; 21(23): 5337–41